Profiling Metabolites through Chemometric Analysis in *Orthosiphon aristatus* Extracts as α-Glucosidase Inhibitory Activity and *In Silico* Molecular Docking

Faizal Maulana[1], Alfari Andiqa Muhammad[2], Ali Umar[1], Fachrur Rizal Mahendra[2], Muhammad Musthofa[2], and Waras Nurcholis[2,3*]

[1]*Department of Chemistry, Faculty of Mathematics and Natural Sciences, IPB University, Jl. Tanjung Kampus IPB Dramaga, Bogor 16680, Indonesia*

[2]*Department of Biochemistry, Faculty of Mathematics and Natural Sciences, IPB University, Jl. Tanjung Kampus IPB Dramaga, Bogor 16680, Indonesia*

[3]*Tropical Biopharmaca Research Center, IPB University, Jl. Taman Kencana Kampus IPB Taman Kencana, Bogor 16128, Indonesia*

Abstract: Orthosiphon aristatus *(called kumis kucing in Indonesia) is a valuable herb for diabetes mellitus treatment. In this study, LC-MS/MS and PCA analyses were used to investigate the metabolite profile, classify* O. aristatus *extracts, and assess the inhibitory activity of α-glucosidase and the probable bioactive compounds through* in silico *study. Results showed that the methanol and ethanol extracts of* O. aristatus *were active in α-glucosidase inhibitory activity. Both extracts contained 86 compounds as known from the LC-MS/MS analysis. PCA analysis identified 10 metabolites that correlated with α-glucosidase inhibitory activity. Results of* in silico *analysis obtained rosmarinic acid compound potentially act as anti-diabetic activity, which can be developed for further research.*

Keywords: *diabetic;* in silico*; Orthosiphon aristatus; metabolomics; PCA*

■ INTRODUCTION

The International Diabetes Federation reported that in 2019, 463 million people were suffering from diabetes mellitus (DM) in the world. It is predicted that this number will continue to increase to reach 700 million people by 2045 [1]. Indonesia's position is in the top 10 under China, America, Pakistan, Brazil, and Mexico. The population of Indonesian people affected by DM is 10.7 million people. According to the Ministry of Health of the Republic of Indonesia, DM is the number 3 cause of death in Indonesia [2]. Even so, about 30–50% of diabetics are not aware of it [3], so the disease condition develops into complications, such as nephropathy [4], cardiovascular [5], gangrene, or impaired wound healing, to stroke [6]. DM is divided into two, namely, type 1 DM and type 2 DM. Type 1 DM occurs due to damage to the β-pancreatic cells that cannot produce insulin properly. In contrast, type 2 DM is caused by the ineffectiveness of the insulin hormone production process.

DM conditions can be determined by calculating blood sugar levels that exceed normal conditions (hyperglycemia). The chronic phase of hyperglycemia causes some of the glucose to undergo auto-oxidation. Glucose auto-oxidation creates reactive oxygen species that act as free radicals, significantly affecting vascular endothelial disorders and leading to complications [7-8]. One way to prevent hyperglycemia is to inhibit the α-glucosidase enzyme [9]. Determination of the target of α-glucosidase enzymes has been commonly used, and several drugs that have been developed are acarbose and voglibose. However, there are reported adverse effects from the usage of the standard drugs, namely gastrointestinal disturbances in diarrhea, dizziness, nausea, vomiting, liver disorders, and central nervous system disorders [10-11]. Therefore, alternative

compounds are needed that can inhibit the activity of the α-glucosidase enzyme.

It was known that bioactive compounds from plants are able to prevent diabetes due to fewer side effects [12]. One of the plants with antioxidant activity tested for α-glucosidase inhibition activity is *Orthosiphon aristatus*. Research from Mohamed et al. [13] has proven the antidiabetic activity of *O. aristatus* by *in vitro* study against the α-glucosidase enzyme. Sinensetin is thought to play a role in the inhibitory activity of *O. aristatus* extract. Although a lot of *O. aristatus*-based research has been performed, a clear classification of the natural compounds based on their polarity and α-glucosidase inhibition activity has not been established. In addition, there may also be other active compounds in *O. aristatus* leaves that have antidiabetic activity, inducing insulin secretion. Based on this research, further investigations are needed to determine the bioactive compounds that play a role in the antidiabetic activity of *O. aristatus*. A metabolomics approach based on a statistical analysis of chemometric complex datasets can be used to obtain information on the role of active chemical compounds [14-16].

This study used Principal Component Analysis (PCA) as the chemometric technique. PCA is a multivariate approach to analyze data tables where many correlated quantitative dependent variables determine observations. The aim is to extract important information from statistical data, express it as a new set of orthogonal variables called principal components, and visualize patterns of similarity between observations and variables [17]. By reducing the number of variables, PCA helps overcome the problem of data overfitting. PCA generates many variations, which will help visualize the data while eliminating related factors such as noise and outliers that have nothing to do with the data. Furthermore, the best compounds that act as the antidiabetic agent will be searched using *in silico* studies. Therefore, the purpose of this research was to determine the metabolite profile of the methanol and ethanol extracts of the *O. aristatus* using LC-MS/MS, classify them using PCA, to determine the inhibitory activity of α-glucosidase, and to study the potential active compounds of *O. aristatus* by *in silico* approach.

■ EXPERIMENTAL SECTION

Research Time and Location

This research was carried out in August–October 2021. This type of research is empirical research in blended activities, online and offline. Offline activities at the IPB Leadership Dormitory, Food Process Engineering laboratory, Tropical Biopharmaca Research Center (Trop-BRC), and IPB Advanced Laboratory and online using supporting media such as WhatsApp, zoom, and google meet applications for three months.

Materials

The main ingredients used in this study were *O. aristatus* powder consisting of leaves, twigs, and flowers obtained from Trop-BRC in powder form, *O. aristatus* compound ligands, filter paper, ethanol, methanol, KH_2PO_4, $KHPO_4$, *p*-nitrophenyl-α-D-glucopyranoside, dimethylsulfoxide (DMSO), acarbose, sodium carbonate, α-glucosidase enzyme, PTFE membrane filter, aquades, and three-dimensional structure of α-glucosidase enzyme (PDB 2QMJ).

Instrumentation

The tools used in this research are cabinet dryer, blender, freezer, rotary evaporator, freeze dryer, 100 mL beaker, 250 and 500 mL Erlenmeyer flasks, stir bar, funnel, analytical balance, incubator, microplate reader, LC-MS/MS (Liquid Chromatography-Mass Spectrometry/Mass Spectrometry) UHPLC Vanquish Tandem Q Exactive Plus Orbitrap HRMS (ThermoScientific, Germany), computer set, software e.g., YASARA Structure, Discovery Studio Visualizer, Avogadro, and PyMol.

Procedure

O. aristatus *extraction*

O. aristatus powder from Trop-BRC will be stored in the freezer until extraction is carried out. Extraction simplicia *O. aristatus* (50 g) 6 samples with each 3 to solvent of ethanol and methanol is made by the method of maceration add solvent until the tera in Erlenmeyer flasks of 250 mL. The mouth of the flask was covered with aluminium foil and then allowed to stand for one

day. Furthermore, the filtrate is filtered. Extraction was repeated three times (triplo). The extract is concentrated with a rotary evaporator. The results of the concentration are then weighed and separated into different vials.

α-Glucosidase enzyme activity inhibition test

Procedure modified from Aziz et al. [18]. A total of 50 μL 0.1 M phosphate buffer pH 6.9, 25 μL *p*-nitrophenyl-α-D-glucopyranoside solution (dissolved in 0.1 M phosphate buffer pH 6.9), 10 μL *O. aristatus* extract was dissolved in DMSO. Acarbose as a positive control was dissolved in distilled water, 25 μL α-glucosidase 0.04 U/mL in 0.1 M buffer solution pH 6.9 was mixed. This reaction was incubated at 37 °C for 30 min. The reaction was stopped by adding 100 μL of 0.2 M sodium carbonate solution. The enzymatic hydrolysis reaction was measured at a wavelength of 410 nm using a microplate reader. The test was carried out two times. The α-glucosidase inhibitory activity was expressed as percent inhibition and was calculated as follows:

$$\% \text{ Inhibition} = \frac{\left[\left(AB - ACS \right) - \left(AS - ACS \right) \right]}{\left(AB - ACB \right)} \times 100\%$$

whereas AB = absorbance of the blank, ACB = absorbance of control blank, AS = absorbance of the sample, and ACS = absorbance of the control sample.

Identification of O. aristatus extract compounds with LC-MS/MS and PCA multivariate data analysis

Procedure modified from Elhawary et al. [19]. A total of 10 mg of sample extract was dissolved in 5 mL of LC-MS/MS grade methanol. The extract dissolution process was carried out with an ultrasonicator for 30 min at room temperature. Then the solution was filtered using a 0.2 μm PTFE filter membrane, and 5 μL of the filtrate was injected in LC-MS/MS. The composition of the mobile phase is adjusted to the best composition of the mobile phase. Raw data *.RAW analysis results from LC-MS/MS can be processed with Compound Discoverer 3.2. After processing, identification was carried out by matching the MS and MS2 spectra of the analyzed compounds with online databases (PubChem, ChemSpider, HMDB, and literature).

The *O. aristatus* extract whose metabolites have been identified are then classified based on the solvent using PCA. The peak area values of the 86 identified compounds were used as variables. The data were imported into excel form, then transposed on the data. After that, they were pre-processed in a center and scaled on the transposed data. Center and scale data are grouped using PCA to obtain at least 70% of the two PCs. The results of the identification of compounds that have been carried out will be continued by *in silico* studies to see the compounds with the most potential as antidiabetics associated with *in vitro*.

In silico *studies*

Procedure modified from Rather et al., Zafar et al., Krieger and Vriend [20-22]. The protein used has a PDB code of 2QMJ with a resolution of 1.90 Å, with a natural ligand on the catalytic site in the form of a complex molecule of acarbose with *N*-acetylglucosamine. Receptor preparation by adding hydrogen atoms, removing water molecules, and not using ligands was carried out using the YASARA Structure software. Then the grid box validation was carried out by redocking 999 times against the 2QMJ receptor until the best grid box validation was obtained at 3 Å. Ligand preparation is done by minimizing the bond energy of the ligand molecules by adding solvent molecules (water) in the system, then saving the files in *.pdb and *.sdf formats. After that, all ligands were collected in one *.sdf file as input for virtual screening with menus (join > object) and atomic coordinates equalization with menus (transfer > all).

After obtaining the best gridbox size from the structure (Table 1), a screening analysis of the *O. aristatus* test ligand was carried out for the receptor. The molecular screening method is carried out by preparing the *_receptor.sce and *_complex.sce files and then preparing the dock_runscreening file with *.mcr format as the command to run the screening process. The prepared ligand file is uploaded before starting the virtual screening process. From virtual screening analysis, the ligands which have higher affinity energy than acarbose was taken. Pharmacokinetic predictions can be made on the webserver provider http://biosig.unimelb.edu.au/pkcsm/prediction_single/ adme_1633876478.78.

Table 1. Gridbox area and binding energy

Gridbox (Å)	Binding energy (kcal/mol)
1	1.668
1.5	1.806
2	2.673
2.5	2.276
3	3.216
3.5	-8.259

Molecular docking using YASARA Structure software. The protein and ligand docking process were carried out 100 times to obtain *.yob and *.txt files containing free energy values (ΔG), inhibition constants (Ki), and amino acid residues. The analysis of the docking results was carried out by comparing the highest free energy, the value of the inhibition constant, and the interaction of amino acid residues using excel. Analysis of bond types using Discovery Studio Visualizer software and 3D visualization using PyMol software.

Data analysis

The data was collected primary data obtained from research and research in the laboratory and computationally. The problems found were analyzed qualitatively and quantitatively based on the results of data collection. Quantitative data were obtained and analyzed from *in silico* data and LC-MS/MS instruments. Qualitative data were analyzed to determine the *O. aristatus* active compounds that potentially as an inhibitor of α-glucosidase. The data is processed, and then conclusions are drawn from the results of the study.

■ **RESULTS AND DISCUSSION**

O. aristatus Extract

This study used ethanol and methanol as solvents to compare the types of compounds dissolved in 2 different organic solvents. Based on the data below, it can be concluded that the ethanol and methanol extracts of herbal formulations started with simplicia weights approaching 50 g. The simplicia was then macerated in ethanol and methanol in a 250 mL volumetric flask. The weight of the extract obtained from the ethanol solvent is shown in Table 2.

α-Glucosidase Enzyme Inhibition

Percent inhibition of *O. aristatus* extract is shown in Table 3 for various concentrations. *In vitro* results shown in Fig. 1 showed that the higher the concentration, the higher the inhibition percentage. Differences can influence these results in geographical origin where they grow, the type of solvent, and the part of the plant used to affect the bioactive content to cause differences in the biological activity of the *O. aristatus* plant [23]. The percentage yield that is not too high can be caused by the extract used being still in a crude form where there are still many compounds in the extract. The use of methanol as a solvent for the extraction of the *O. aristatus* plant is known to extract more active compounds and has a higher phytochemical constituent as well as total phenolic content than other solvents [24].

Table 2. Extract yield with ethanol and methanol solvent

Label	Simplicia weight (g)	Extract weight (g)	% Yield
E1	50.01	2.54	5.08
E2	49.78	2.52	5.07
E3	49.78	3.58	7.17
M1	50.01	3.42	6.83
M2	50.16	3.70	7.38
M3	49.96	3.36	6.73

Table 3. %Inhibition of *O. aristatus* extract

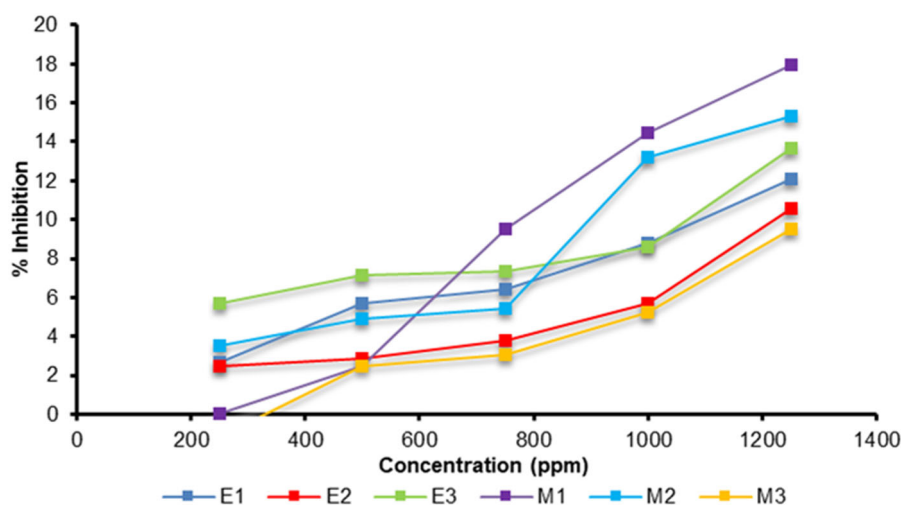| Concentration (ppm)	%Inhibition					
	E1	E2	E3	M1	M2	M3
1250	12.096	10.603	13.650	17.946	15.296	9.537
1000	8.775	5.728	8.592	14.473	13.193	5.210
750	6.399	3.778	7.313	9.537	5.424	3.077
500	5.667	2.864	7.130	2.468	4.906	2.468
250	2.651	2.438	5.698	0.030	3.504	-1.158

Fig 1. Graph of % inhibition at all concentrations

O. aristatus plant is rich in phenolic compounds, including flavonoids [25]. Some literatures stated that compounds inhibiting the activity of α-glucosidase belong to this group [26]. Therefore, in the next stage, metabolite analysis of ethanol and methanol extracts was carried out to see the differences in the content of the compounds by classifying them using PCA, which would then look for compounds that play a role in α-glucosidase inhibition in the *in silico* study.

Compound Profile and PCA Classification

LC-MS/MS is an analytical technique that combines the separation capabilities of liquid chromatography with the specificity of mass spectrophotometric detection. Data in the form of chromatograms of each plant sample based on different solvents were combined into a chromatogram as shown in Fig. 2. The results of the chromatograms have different patterns, which explain the differences in the composition of compounds detected in each solvent. The chromatogram was processed using Compound Discoverer software and obtained 86 compounds identified in the *O. aristatus* plant extract with various solvents. These compounds result from MS-MS fragmentation compared with the literature, so the identification of these components is putative. These compounds consist of alkaloids, phenolic acids, flavonoids, coumarins, steroids, and other group compounds (Table 4).

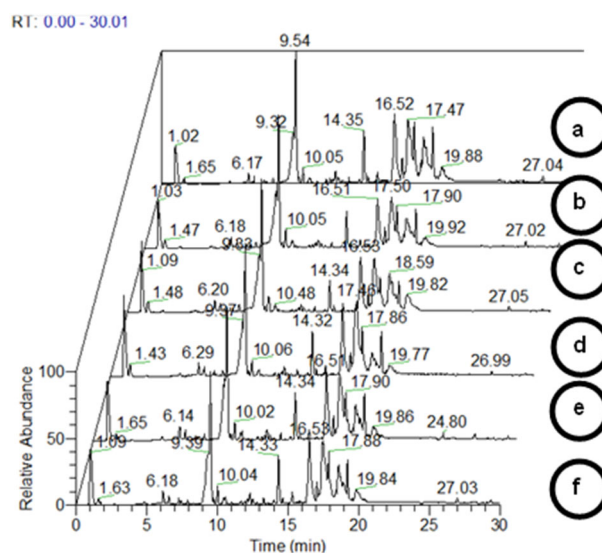Analysis with PCA aims to summarize complex data

Fig 2. LC-MS/MS chromatogram results, (a) E1, (b) E2, (c) E3, (d) M1, (e) M2, (f) M3

and show the variance and how the sample is different from other samples. Cluster formation on a particular PC is the most influential function in this analysis. The PCA score plot shows the grouping of each sample based on the variable peak area of the chromatogram (Fig. 3(a)). This PCA analysis aims to see that the metabolite profile of each sample can be distinguished by solvent. The most frequently used components in PCA analysis are component 1 (PC1) and component 2 (PC2). The plot of scores generated from this study resulted in a diversity of data from both PCs of 70.3%. This shows that 70.3% of the data diversity can be explained by the

Table 4. *O. aristatus* compound identification using LC-MS/MS

Peak	Compound	Formula	Molecular weight	Rt [min]	E1	E2	E3	M1	M2	M3
1	3-Amino-2,3-dideoxy-scyllo-inosose	$C_6H_{11}NO_4$	161.06868	1.003	√	√	√		√	√
2	Kanosamine	$C_6H_{13}NO_5$	179.07926	1.004	√	√	√	√	√	√
3	Linamarin	$C_{10}H_{17}NO_6$	247.10535	1.025		√	√	√	√	
4	γ-Aminobutyric acid	$C_4H_9NO_2$	103.06354	1.028	√	√	√	√	√	
5	*N*-Acetyl-L-ornithine	$C_7H_{14}N_2O_3$	174.10029	1.036	√	√	√	√	√	√
6	Adenosine	$C_{10}H_{13}N_5O_4$	267.09610	1.039	√			√	√	√
7	Lotaustralin	$C_{11}H_{19}NO_6$	261.12114	1.040		√	√		√	√
8	Cytidine	$C_9H_{13}N_3O_5$	243.08537	1.045		√				
9	L-glutamine	$C_5H_{10}N_2O_3$	146.06902	1.048		√				
10	5-Oxo-L-proline	$C_5H_7NO_3$	129.04262	1.050		√		√		
11	5-aminopentanoate	$C_5H_{11}NO_2$	117.07900	1.055	√	√	√	√	√	√
12	*N*-Dimethylethanolamine phosphate	$C_4H_{12}NO_4P$	169.05042	1.060					√	
13	3,6-dihydronicotinate	$C_6H_7NO_2$	125.04767	1.063	√	√	√	√	√	√
14	Phenylglyoxylate	$C_8H_6O_3$	150.03147	1.106	√					
15	(R)-1-Amino-2-propanol O-2-phosphate	$C_3H_{10}NO_4P$	155.03477	1.106	√		√	√		√
16	Adenine	$C_5H_5N_5$	135.05442	1.120		√				√
17	Sucrose	$C_{12}H_{22}O_{11}$	359.14216	1.174	√	√	√	√	√	√
18	4-O-Acetyl-*N*-acetylmannosamine	$C_{10}H_{17}NO_7$	263.10034	1.227	√	√		√	√	
19	Nicotinic acid	$C_6H_5NO_2$	123.03207	1.316	√	√	√	√	√	
20	Uridine	$C_9H_{12}N_2O_6$	244.06926	1.385				√		
21	Uracil	$C_4H_4N_2O_2$	112.02753	1.387		√				
22	L-Pyroglutamic acid	$C_5H_7NO_3$	129.04253	1.387	√			√	√	√
23	Adenine	$C_5H_5N_5$	135.05442	1.389	√				√	
24	Adenosine	$C_{10}H_{13}N_5O_4$	267.09617	1.402		√	√	√		√
25	L-tyrosine	$C_9H_{11}NO_3$	181.07388	1.440	√	√	√	√		
26	L-isoleucine	$C_6H_{13}NO_2$	131.09453	1.549	√	√	√	√	√	√
27	Adenine	$C_5H_5N_5$	135.05446	1.551					√	√
28	Adenosine	$C_{10}H_{13}N_5O_4$	267.09612	1.573	√				√	√
29	(S)-2-Amino-6-oxohexanoate	$C_6H_{11}NO_3$	145.07370	1.599	√	√	√	√	√	
30	D-proline	$C_5H_9NO_2$	115.06341	1.727	√	√	√	√	√	√
31	L-pipecolate	$C_6H_{11}NO_2$	129.07898	1.853	√	√	√	√	√	√
32	L-phenylalanine	$C_9H_{11}NO_2$	165.07884	2.130	√	√	√		√	
33	Pantothenate	$C_9H_{17}NO_5$	219.11060	2.411					√	
34	L-tryptophan	$C_{11}H_{12}N_2O_2$	204.08970	4.307	√	√	√			
35	Kynurenate	$C_{10}H_7NO_3$	189.04246	4.878	√	√		√	√	√
36	Kaempferol 7-O-glucoside	$C_{21}H_{20}O_{11}$	448.09977	7.763	√	√	√	√	√	√
37	Methyl eugenol	$C_{11}H_{14}O_2$	178.09932	8.648						√
38	Kaempferol 7-O-glucoside	$C_{21}H_{20}O_{11}$	448.09963	8.985	√	√	√	√	√	√
39	Caffeic acid	$C_9H_8O_4$	180.04188	9.526	√	√	√	√	√	√
40	Rosmarinic acid	$C_{18}H_{16}O_8$	360.08328	9.528	√	√	√	√	√	√
41	Umbelliferone	$C_9H_6O_3$	162.03130	9.529	√	√	√	√	√	√
42	Versiconal	$C_{18}H_{14}O_8$	358.06844	9.978	√	√	√	√	√	√
43	Versicolorin B	$C_{18}H_{12}O_7$	340.05786	9.978	√	√	√	√	√	√
44	Salvianolic acid B	$C_{36}H_{30}O_{16}$	718.15274	10.050	√	√	√	√	√	√
45	Damascenone	$C_{13}H_{18}O$	190.13564	11.020	√	√	√	√		√
46	Kaempferol	$C_{15}H_{10}O_6$	286.04750	12.470		√				
47	5-Hydroxy-6,7,3',4'-tetramethoxyflavone	$C_{19}H_{18}O_7$	358.10407	12.595	√	√	√	√	√	√
48	(3r)-sophorol	$C_{16}H_{12}O_6$	300.06291	13.884	√	√				
49	Sinensetin	$C_{20}H_{20}O_7$	372.11952	14.021	√	√	√	√	√	√
50	2-hydroxyformononetin	$C_{16}H_{12}O_5$	284.06786	14.265		√	√			

Table 4. *O. aristatus* compound identification using LC-MS/MS (*Continued*)

Peak	Compound	Formula	Molecular weight	Rt [min]	E1	E2	E3	M1	M2	M3
51	Eupatorin	$C_{18}H_{16}O_7$	344.08837	14.347	√	√	√	√	√	√
52	Aflatoxin B2	$C_{17}H_{14}O_6$	314.07792	14.474	√	√	√	√	√	√
53	Scutellarein 5,6,7,4'-tetramethyl ether	$C_{19}H_{18}O_6$	342.10913	15.143	√	√	√	√	√	√
54	(1's,5's)-hydroxyaverantin	$C_{20}H_{20}O_8$	388.11527	15.307	√	√				√
55	Gibberellin A36	$C_{20}H_{26}O_6$	362.17207	15.309	√	√	√	√	√	√
56	2-hydroxyformononetin	$C_{16}H_{12}O_5$	284.06801	15.402	√	√				√
57	Aflatoxin G2	$C_{17}H_{14}O_7$	330.07303	15.863	√	√	√	√	√	√
58	(9s)-hpode	$C_{18}H_{32}O_4$	312.22963	15.896	√	√				
59	Curcumin	$C_{21}H_{20}O_6$	368.12532	16.376	√					
60	Hyperxanthone E	$C_{18}H_{16}O_6$	328.09345	17.378	√	√	√	√	√	√
61	Orthosiphols R	$C_{36}H_{42}O_{10}$	634.27567	17.600	√	√		√	√	√
62	Neoorthosiphol A	$C_{38}H_{44}O_{12}$	692.28068	17.714	√	√		√	√	
63	Gibberellin A24	$C_{20}H_{26}O_5$	346.17718	17.903	√		√	√	√	√
64	Orthosiphols S	$C_{34}H_{36}O_9$	588.23481	18.363	√	√	√	√	√	√
65	Norstaminols C	$C_{30}H_{36}O_{10}$	556.22938	18.375	√	√	√	√	√	√
66	Norstaminolactone A	$C_{38}H_{45}NO_{12}$	707.29349	18.736		√		√	√	√
67	Estrone	$C_{18}H_{22}O_2$	270.16144	18.854	√	√	√	√	√	√
68	Androsta-1,4-diene-3,17-dione	$C_{19}H_{24}O_2$	284.17705	18.854	√	√	√	√	√	√
69	Indole	C_8H_7N	117.05784	19.233	√	√	√	√		√
70	Orthosiphonone A	$C_{38}H_{42}O_{11}$	674.27064	19.235	√	√	√	√	√	√
71	9α-Hydroxyandrosta-1,4-diene-3,17-dione	$C_{19}H_{24}O_3$	300.17193	19.236	√	√	√	√	√	√
72	9,10-Epoxy-10,12Z,15Z-octadecatrienoate	$C_{18}H_{28}O_3$	292.20319	19.323	√	√	√	√	√	√
73	Demethylphylloquinone	$C_{30}H_{44}O_2$	436.33339	19.437	√	√	√	√	√	√
74	β-Ionone	$C_{13}H_{20}O$	192.15125	19.659	√	√	√	√	√	√
75	A-Linolenate	$C_{18}H_{30}O_2$	278.22398	19.696	√	√	√	√	√	√
76	Colneleate	$C_{18}H_{30}O_3$	294.21877	20.283	√	√	√	√	√	√
77	Hydroxybetulinic acid	$C_{30}H_{48}O_4$	472.35439	20.347	√	√	√	√	√	√
78	17-β-Hydroxy-5-α-androstan-3-one	$C_{19}H_{30}O_2$	290.22392	21.901	√	√	√	√	√	√
79	4α-Hydroxymethyl-4β-methyl-5α-cholesta-8,24-dien-3β-ol	$C_{29}H_{48}O_2$	428.36455	24.347		√				
80	Violaxanthin	$C_{40}H_{56}O_4$	600.41643	24.464	√	√				
81	4,4-Dimethyl-cholesta-8,12,24-trienol	$C_{29}H_{46}O$	410.35380	24.514	√	√	√	√	√	
82	Linoleate	$C_{18}H_{32}O_2$	280.23965	25.427	√	√				
83	Ent-kaurene	$C_{20}H_{32}$	272.24986	26.009	√	√	√	√	√	√
84	Cycloeucalenone	$C_{30}H_{48}O$	424.36959	26.353	√	√	√	√	√	√
85	14-hydroxylanosterol	$C_{30}H_{50}O_2$	442.38044	26.353	√	√			√	√
86	4α-Hydroxymethyl-4β-methyl-5α-cholesta-8,24-dien-3β-ol	$C_{29}H_{48}O_2$	428.36391	27.260				√		

Rt: Retention time in min

E1: Ethanol sample 1   M1: Methanol sample 1
E2: Ethanol sample 2   M2: Methanol sample 2
E3: Ethanol sample 3   M3: Methanol sample 3

variable area of the peak chromatogram of *O. aristatus* plant based on the solvent. The value of the two PCs shows a fairly good two-dimensional visualization because the diversity value of PC1 and PC2 is greater than 70% [27].

Biplot of the PCA is a multivariate method that uses rows and columns in a chart. This method displays the object and the variables with the object under study [28]. Based on Fig. 3(b), the compound that plays a role in the inhibitory activity of α-glucosidase is the number
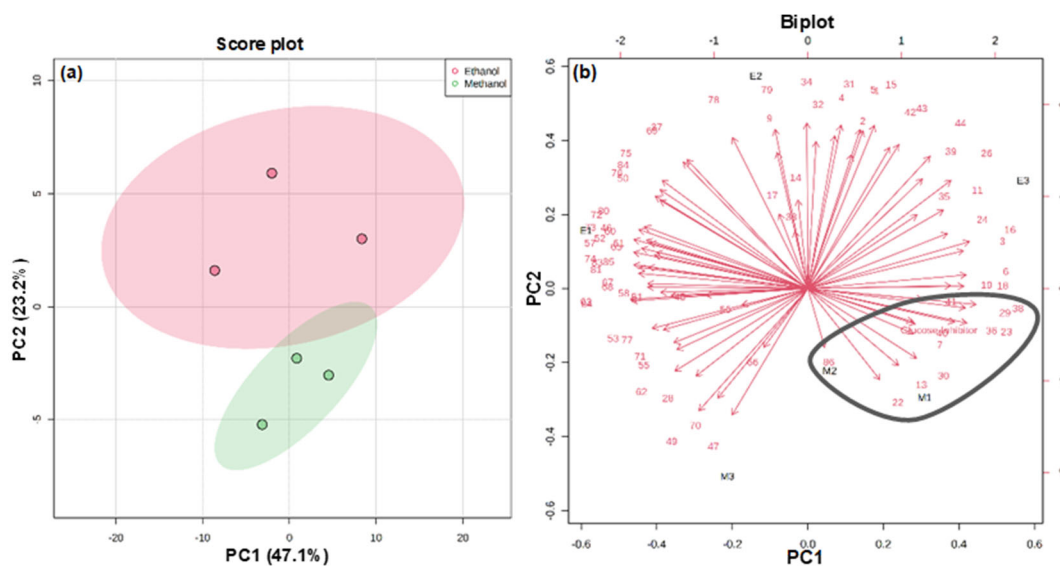
Fig 3. PCA results, (a) Score plot, (b) Biplot

Table 5. Virtual screening of *O. aristatus* extract

No.	Ligands	Effi [kcal/(mol*Atom)]	Bind. energy [kcal/mol]	Dissoc. constant [μM]
1	Rosmarinic acid	0.3153	8.197	0.01
2	Kaemferol 7-O-glucoside	0.2521	8.066	0.98
3	Acarbose	0.1770	7.787	1.96
3	4α-Hydroxymethyl-4β-methyl-5α-cholesta-8,24-dien-3β-ol	0.2266	7.025	7.08
5	Uridine	0.3882	6.599	14.50
6	Umbelliferone	0.5126	6.151	30.99
7	5-Oxo-L-proline	0.6683	6.015	38.89
8	(S)-2-Amino-6-oxohexanoate	0.5849	5.849	51.59
9	Nicotinic acid	0.6216	5.594	79.34
10	Lotaustralin	0.3102	5.584	80.70

of compounds that approach glucose inhibitors. The number of compounds that can be seen on the document the results of the identification of compound LC-MS/MS (Table 5) with 10 compounds. The tenth compounds further studies will be carried out *in silico*.

In silico Study

Receptor protein structure stability

The structure of the receptor used in this study is a complex of α-glucosidase and acarbose enzymes with the code 2QMJ. The technique used to determine the 3D structure of this enzyme is X-ray diffraction with a resolution value of 1.90, which is relatively high [29]. The following analysis is the stability of the receptor. The analysis carried out on the PROCHECK page produces a Ramachandran plot with the percentage of residues in quadrant I (most favored regions) of 87.2% with 654 residues, quadrant II (additional allowed regions) of 11.6% with 87 residues, quadrant III (generously allowed regions) of 0.8% with six residues, and quadrant IV (disallowed regions) of 0.4% with three residues. The quality of the protein structure is said to be good if it has a percentage of residues in the preferred region > 90% [28].

Grid box validation

Validation of the 2QMJ receptor was carried out by first cleaning water and natural ligands attached to its structure, such as sulfate ions and glycerol. Acarbose (AC1) binds to *N*-acetyl D-glucosamine to form an

inhibitor complex used as a comparison. AC1 and *N*-acetyl-D-glucosamine, which have been attached to the receptor, are separated and prepared. The anchoring validation was carried out by re-docking the complex molecule of AC1 and *N*-acetyl-D-glucosamine to the enzyme 999 times, and the best pose was taken. Validation was carried out by testing the molecular anchoring of the grid box from size 1 to 5 Å. The increase in grid box size was based on an interval value of 0.5 Å. The highest affinity energy value was obtained when the grid box size was 3 Å.

Virtual screening

The inhibition constant is proportional to the bond free energy value, the greater the bond free energy value, the greater the inhibition constant and vice versa. The value of the binding free energy and the inhibition constant obtained by each ligand is influenced by the interaction between the ligand and the receptor [30]. Therefore, visualization of molecular docking was carried out to determine the various types of interactions with amino acid residues. In addition, there is a ligand

efficiency parameter that interprets the ratio of the average binding energy value per atom obtained from the free Gibbs energy divided by the number of atomic weights (LE = -ΔG/N) with units of (kcal/(mol.Atom)). Fragments with the high-efficiency value of ligand are directly proportional to the strength of the binding affinity of the ligand and receptor to guide the discovery of potential compounds [31].

Virtual screening with the YASARA structure filters and determines the interaction between ligands and receptors as drug candidates. Two ligand identifiers that have the best results against acarbose are kaempferol 7-O-glucoside and rosmarinic acid. The binding energy value (ΔG) of rosmarinic acid, kaempferol 7-O-glucoside, and acarbose was 8.197, 8.066, and 7.787 kcal/mol, respectively. In addition, the obtained values of Ki of each of 0.0081, 0.980, and 1.9595 μM, and the value of the efficiency of the ligand respectively 0.3153, 0.2521, and 0.177 kcal/(mol*Atom), respectively.

Acarbose as a ligand comparison has interactions with amino acid side active, i.e., Tyr299, Asp327, Asp443,
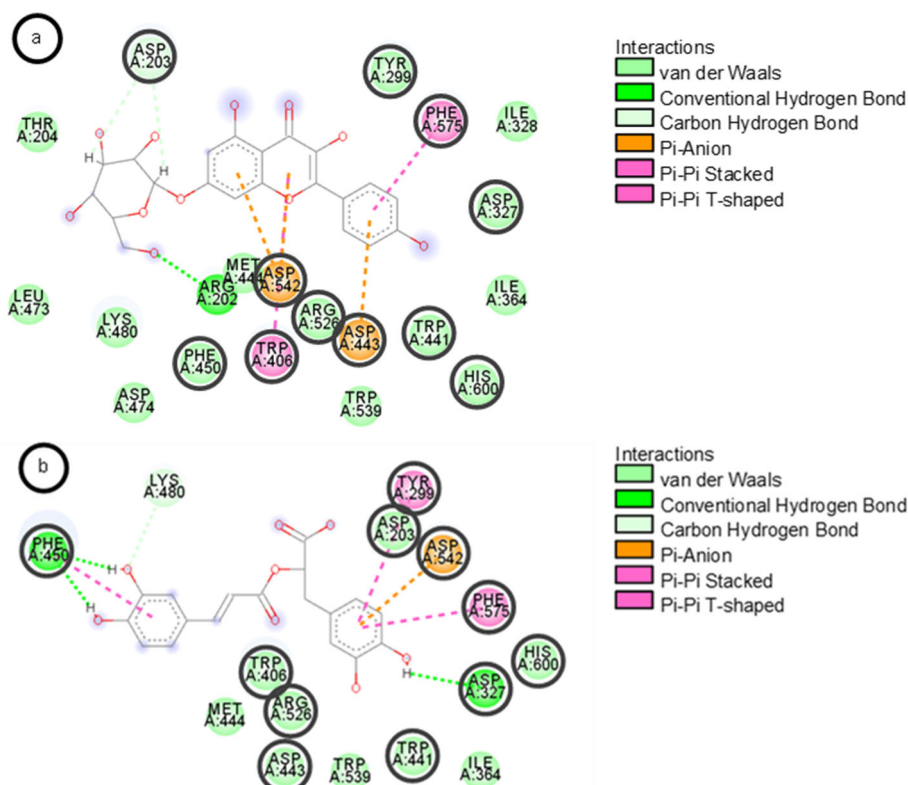

Fig 4. Amino acid residue, (a) kaempferol 7-O-glucoside, (b) rosmarinic acid, (c) acarbose
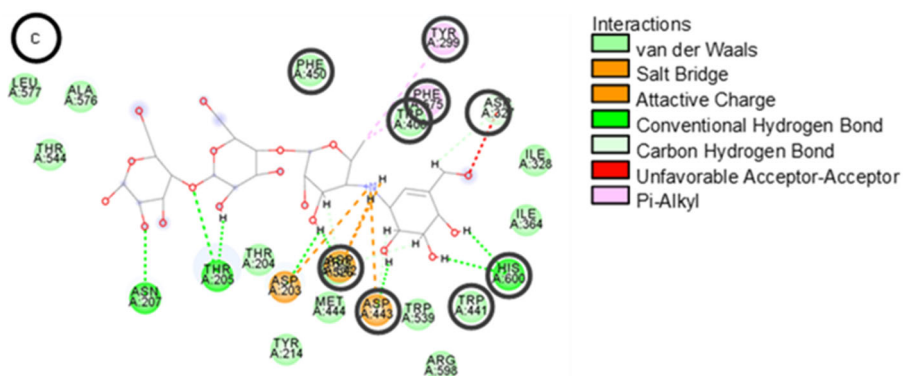
Fig 4. Amino acid residue, (a) kaempferol 7-O-glucoside, (b) rosmarinic acid, (c) acarbose (*Continued*)
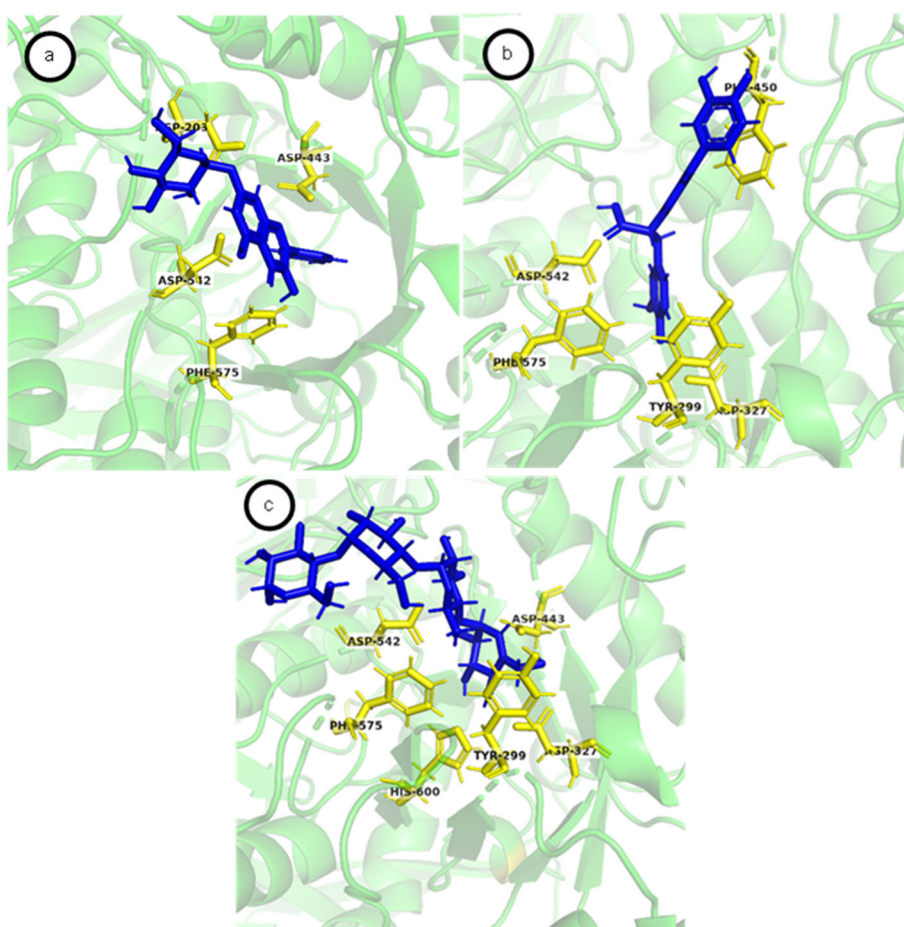

Fig. 5. 3D structure of α-GOX, (a) kaempferol 7-O-glucoside, (b) rosmarinic acid, (c) acarbose

Asp542, Phe575, His600 (hydrogen bond) and Trp406, Trp441, Phe450, Arg526 (Van der Waals bond). Rosmarinic acid interacts with residues Tyr299, Asp327, Phe450, Asp542, Phe575 (hydrogen bond) and Asp203, Trp406, Trp441, Asp443, Arg526, His600 (Van der Waals bond) (Fig. 4(b)). Kaempferol 7-O-glucoside interacts with

residues Asp203, Asp443, Asp542, Phe575 (hydrogen bond) and Tyr299, Asp327, Trp406, Trp441, Phe450, Arg526, His600 (Van der Waals bond) (Fig. 4(a)). This interaction is also presented in 3D, as shown in Fig. 5.

The correlation analysis between binding energy, inhibition constant, and ligand efficiency as shown in

Indones. J. Chem., 2022, 22 (2), 501 - 514

511

Fig. 6 shows a negative correlation (purple color) between the binding energy value and the inhibition constant. Still, there was no correlation whatsoever to the efficiency value. This is because many other factors are involved in determining the value of the efficiency of the ligand, such as the number of atomic weights in the ligand [31].

Regression analysis showed a correlation between the binding energy of the ligands and the inhibition constant (Fig. 7). The decrease in the value of the inhibition constant is inversely proportional to the increase in the binding energy of the ligand, so the smaller the value of the inhibition constant indicates the stronger the ligand is attached to the receptor and vice versa, the greater the inhibition constant, the weaker the ligand is bound to the receptor. This result is in accordance with the research by Iman and Saadabadi [30].

Ligand bioavailability analysis

The two best compounds, rosmarinic acid and kaempferol 7-O-glucoside were analyzed bioavailability is based on the rules of Lipinski [32]. Five parameters that are used, among others, molecular weight ≤ 500 Da, hydrogen acceptors ≤ 10, hydrogen donors ≤ 5, log P ≤ 5, the value of PSA ≤ 140 A, and the number of rotatable bonds ≤ 10 [33-34]. On pharmacokinetic analysis, the ligand that violates more than two rules of Lipinski otherwise does not qualify and does not proceed to subsequent analysis [35]. In addition, the ligand with a value of Log P < 0 marked shows the value of which is less than ideal in the rules of Lipinski, so that did not pass the test analysis of the pharmacokinetic [36].

Rosmarinic acid has a molecular weight of 360 g/mol, hydrogen acceptors 8, hydrogen donors 5, log P value equal to 1.65, the value of PSA 144 A, and the number of the rotatable bond as much as 7. In comparison, kaempferol 7-O-glucoside has a molecular weight of 448 g/mol, hydrogen acceptors 11, donor hydrogen 7, the value of log P -0.23, the value of PSA 190, and rotatable bond as much as 4. Ligand rosmarinic acid violates the rules of Lipinski, while for the ligand kaempferol 7-O-glucoside breaking the Log P ≤ 0, then it is not suitable to be used as an oral drug.

O. aristatus has a high rosmarinic acid content with 53–299 mg/g among other herbal plants [37]. Antidiabetic activity of this compound showed that treatment with rosmarinic acid (120–200 mg/kg) for 7 days fixed the
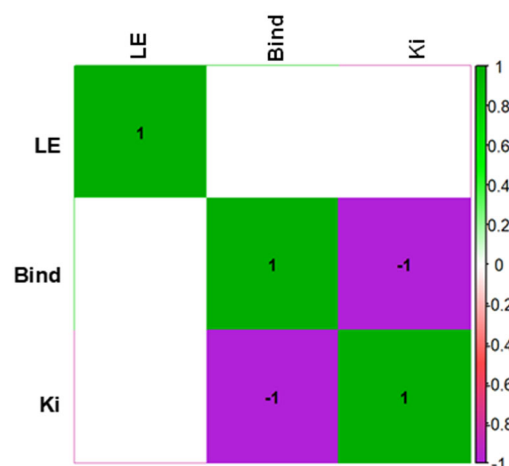
Fig 6. Result of correlation analysis between binding energy (Bind), inhibition constant (Ki), ligand efficiency (LE)

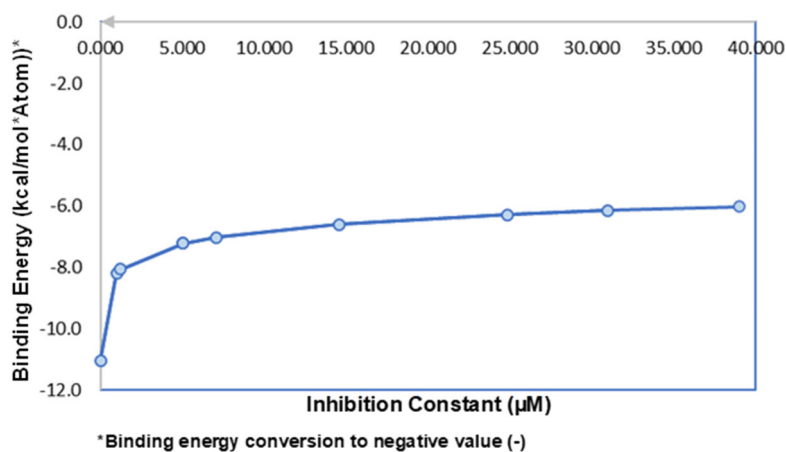*Binding energy conversion to negative value (-)

Fig 7. Regression analysis of binding energy and inhibition constant

hypoglycemic effect of rat type 1 diabetes induced by streptozocin. Experiments also showed an increase in glucose absorption from the 5.71 be about 7.42 mmol/L, and insulin sensitivity from 36.60 to 74.76 μU/mL in mice with type 2 diabetes induced by a high-fat diet [38]. Therefore, the compound rosmarinic acid into compounds of potential developed as a new herbal remedy.

■ **CONCLUSION**

Extracts of *O. aristatus* plant in methanol and ethanol solvents have different compositions of the existing compounds using PCA chemometrics with the diversity of PC data was 70.3%. *O. aristatus* plant is proven to inhibit the activity of the α-glucosidase enzyme. To find the compounds that play a role in the antidiabetic activity, *in silico* test found the best compounds to be developed into a new herbal remedy, namely rosmarinic acid. This study is still in the *in vitro* and *in silico* stages. Therefore, more procedures, such as *in vivo* as pre-clinical and toxicity tests, are required before it can be proceeded into clinical trials.

■ **AUTHOR CONTRIBUTIONS**

Waras Nurcholis conducted design experiment and analysis data, and also revised the manuscript. Alfari Andiqa Muhammad, Ali Umar, Fachrur Rizal Mahendra, and Muhammad Musthofa conducted the experiment, Faizal Maulana conducted the PCA calculations, Fachrur Rizal Mahendra conducted the molecular docking calculations, Alfari Andiqa Muhammad, Ali Umar, and Muhammad Musthofa wrote and revised the manuscript. All authors agreed to the final version of this manuscript.

■ **REFERENCES**

[1] International Diabetes Federation, 2019, *IDF Diabetes Atlas*, 9th Ed., International Diabetes Federation, Belgium.

[2] Aquarista, N.C., 2016, Differences characteristics patients diabetes mellitus type 2 with and without coronary heart disease, *JBE*, 5 (1), 37–47.

[3] Beagley, J., Guariguata, L., Weil, C., and Motala, A.A., 2014, Global estimates of undiagnosed diabetes in adults, *Diabetes Res. Clin. Pract.*, 103 (2), 150–160.

[4] Miranda-Díaz, A.G., Pazarín-Villaseñor, L., Yanowsky-Escatell, F.G., and Andrade-Sierra, J., 2016, Oxidative stress in diabetic nephropathy with early chronic kidney disease, *J. Diabetes Res.*, 2016, 7047238.

[5] Lathifah, N.L., 2017, Hubungan durasi penyakit dan kadar gula darah dengan keluhan subyektif penderita diabetes melitus, *JBE*, 5 (2), 231–239.

[6] Ullah, F., Afridi, A.K., Rahim, F., Ashfaq, M., Khan, S., Shabbier, G., and Ur Rahman, S., 2015, Knowledge of diabetic complication in patients with diabetes mellitus, *J. Ayub Med. Coll. Abbottabad*, 27 (2), 360–363.

[7] Arman, M.S.I., Al Mahmud, A., Mahmud, H.R., and Reza, A.S.M.A., 2019, Free radical, oxidative stress and diabetes mellitus: A mini review, *Discovery Phytomed.*, 6 (3), 99–101.

[8] Tiwari, B.K., Pandey, K.B., Abidi, A.B., and Rizvi, S.I., 2013, Markers of oxidative stress during diabetes mellitus, *J. Biomarkers*, 2013, 378790.

[9] Chatsumpun, N., Sritularak, B., and Likhitwitayawuid, K., 2017, New bioflavonoids with α-glucosidase and pancreatic lipase inhibitory activities from *Boesenbergia rotunda*, *Molecules*, 22 (11), 1862.

[10] Dhabi, A.S., Bhatt, N.R., and Shah, M., 2013, Voglibose: An alpha glucosidase inhibitor, *J. Clin. Diagn. Res.*, 7 (12), 3023–3027.

[11] Hasimun, P., Adnyana, I.K., Valentina, R., and Lisnasari, E., 2016, Potential alpha glucosidase inhibitor from selected zingiberaceae family, *Asian J. Pharm. Clin. Res.*, 9 (1), 164–167.

[12] Yuan, H., Ma, Q., Ye, L., Piao, G., 2016, The traditional medicine and modern from natural products. *Molecules*, 21 (559), 1–18.

[13] Mohamed, E.A.H., Siddqui, M.J.A., Ang, L.F., Sadikun, A., Chan, S.H., Tan, S.C., Asmawi, M.Z., and Yam, M.F., 2012, Potent α-glucosidase and α-amylase inhibitory activities of standardized 50% ethanolic extracts and sinensetin from *Orthosiphon stamineus* Benth as anti-diabetic mechanism, *BMC Complementary Altern. Med.*, 12 (1), 176.

[14] Ashraf, K., Sultan, S., and Adam, A., 2018, *Orthosiphon stamineus* Benth. is an outstanding food medicine: Review of phytochemical and pharmacological activities, *J. Pharm. BioAllied Sci.*, 10 (3), 109–118.

[15] Murugesu, S., Ibrahim, Z., Ahmed, Q.U., Nik Yusoff, N.I., Uzir, B.F., Perumal, V., Abas, F., Saari, K., El-Seedi, H., and Khatib, A., 2018, Characterization of α-glucosidase inhibitors from *Clinacanthus nutans* Lindau leaves by gas chromatography-mass spectrometry-based metabolomics and molecular docking simulation, *Molecules*, 23 (9), 2402.

[16] Guedes, J.A.C., Filho, E.G.A., Silva, M.F.S, Rodrigues, T.H.S., Ramires, C.M.C., Lima, M.A.C., Silva, G.S., Pessoa, C.O., Canuto, K.M., Brito, E.S., Alves, R.E., Nascimento, R.F., and Zocolo, G.J., 2020, GC-MS-based metabolomic profiles combined with chemometric tools and cytotoxic activities of non-polar leaf extract of *Spondias mombin* L. and *Spondias tuberosa* Arr. Cam, *J. Braz. Chem. Soc.*, 31 (2), 331–340.

[17] Mishra, S., Sarkar, U., Taraphder, S., Datta, S., Swain, D.P., Saikhom, R., Panda, S., and Laishram, M., 2017, Multivariate statistical data analysis- Principal component analysis, *Int. J. Livest. Res.*, 7 (5), 60–78.

[18] Aziz, Z., Yuliana, D.N., Simanjuntak, P., Rafi, M., Mulatsari, E., and Abdilah, S., 2021, Investigation of yacon leaves (*Smallanthus sonchifolius*) for α-glucosidase inhibitors using metabolomics and *in silico* approach, *Plant Foods Hum. Nutr.*, 76 (4), 487–493.

[19] Elhawary, S.S., Younis, Y.I., Bishbishy, E.H.M., and Khattab, R.A., 2018, LC-MS/MS-based chemometric analysis of phytochemical diversity in 13 *Ficus* spp. (Moraceae): Correlation to their *in vitro* antimicrobial and *in silico* quorum sensing inhibitory activities, *Ind. Crops Prod.*, 126, 261–271.

[20] Rather, M.A., Dutta, S., Guttula, P.K., Dhandare, B.C., Yusufzai, S.I., and Zafar, M.I., 2020, Structural analysis, molecular docking and molecular dynamics simulations of G-protein-coupled receptor (kisspeptin) in fish, *J. Biomol. Struct. Dyn.*, 38 (8), 2422–2439.

[21] Zafar, M., Khan, H., Rauf, A., Khan, A., and Lodhi, M.A., 2016, *In silico* study of alkaloid as α-glucosidase inhibitors: Hope for the discovery of effective lead compounds, *Front. Endocrinol.*, 7, 153.

[22] Krieger, E., and Vriend, G., 2015, New ways to boost molecular dynamics simulations, *J. Comput. Chem.*, 36 (13), 996–1007.

[23] Rafi, M., Purwakusumah, E.D., Ridwan, T., Barus, B., Sutandi, A., and Darusman, L.K., 2015, Geographical classification of Java tea (*Orthosiphon stamineus*) from Java Island by FTIR spectroscopy combined with canonical variate analysis, *JSM*, 23 (1), 25–31.

[24] Truong, D.H., Nguyen, D.H., Ta, N.T., Bui, A.V., Do, T.H., and Nguyen, H.C., 2019, Evaluation of the use of different solvents for phytochemical constituents, antioxidants, and *in vitro* anti-inflammatory activities of *Severinia buxifolia*, *J. Food Qual.*, 2019, 8178294.

[25] Himani, B., Seema, B., Bhole, N., Mayank, Y., Vinod, S., and Mamta, S., 2013, Misai kuching: A glimpse of maestro, *Int. J. Pharm. Sci. Rev. Res.*, 22 (2), 55–59.

[26] Şöhretoğlu, D., and Sari, S., 2019, Flavonoids as alpha-glucosidase inhibitors: Mechanistic approaches merged with enzyme kinetics and molecular modelling, *Phytochem. Rev.*, 19 (5), 1081–1092.

[27] Jolliffe, I.T., and Cadima, J., 2016, Principal component analysis: A review and recent developments, *Philos. Trans. R. Soc., A*, 374 (2065), 20150202.

[28] Zobayer, N., and Aowlad Hossain, A.B.M., 2018, *In silico* characterization and homology modelling of histamine receptors, *J. Biol. Sci.*, 18 (4), 178–191.

[29] Ueno, G., Shimada, A., Yamashita, E., Hasegawa, K., Kumasaka, T., Shinzawa-Itoh, K., Yoshikawa, S., Tsukihara, T., and Yamamoto, M., 2019, Low-dose X-ray structure analysis of cytochrome c oxidase utilizing high-energy X-rays, *J. Synchrotron Radiat.*, 26 (4), 912–921.

[30] Iman, M., Saadabadi, A., and Davood, A., 2015, Molecular docking analysis and molecular dynamics simulation study of ameltolide analogous as a sodium channel blocker, *Turk. J. Chem.*, 39, 306–316.

[31] Chen, H., Zhou, X., Gao, Y., Chen, H., and Zhou, J., 2017, "Fragment-Based Drug Design: Strategic Advances and Lessons Learned" in *Comprehensive Medicinal Chemistry III*, Eds. Chackalamannil S., Rotella D., Ward S.E., Elsevier, Oxford, 212–232.

[32] Lipinski, C.A., Lombardo, F., Dominy, B.W., and Feeney, P.J., 2012, Experimental and computational approaches to estimate solubility and permeability in drug discovery and development settings, *Adv. Drug Delivery Rev.*, 64 (Suppl.), 4–17.

[33] Bickerton, G.R., Paolini, G.V., Besnard, J., Muresan, S., and Hopkins, A.L., 2012, Quantifying the chemical beauty of drugs, *Nat. Chem.*, 4 (2), 90–98.

[34] Doak, B.C., Over, B., Giordanetto, F., and Kihlberg, J., 2014, Oral druggable space beyond the rule of 5: Insights from drugs and clinical candidates, *Chem. Biol.*, 21 (9), 1115–1142.

[35] Benet, L.Z., Hosey, C.M., Ursu, O., and Oprea, T.I., 2016, BDDCS, the Rule of 5 and drugability, *Adv. Drug Delivery Rev.*, 101, 89–98.

[36] Chagas, C.M., Moss, S., and Alisaraie, L., 2018, Drug metabolites and their effects on the development of adverse reactions: Revisiting Lipinski's Rule of Five, *Int. J. Pharm.*, 549 (1-2), 133–149.

[37] Chua, S.L., Lau, C.H., Chew, C.Y., Ismail, N.I.M., and Sootorgun, N., 2017, Phytochemical profile of *Orthosiphon aristatus* extracts after storage: Rosmarinic acid and other caffeic acid derivatives, *Phytomedicine*, 39, 49–55.

[38] Runtuwene, J., Cheng, K.C., Asakawa, A., Amitani, H., Amitani, M., Morinaga, A., Takimoto, Y., Kairupan, B.H.R., and Inui, A, 2016, Rosmarinic acid ameliorates hyperglycemia and insulin sensitivity in diabetic rats, potentially by modulating the expression of PEPCK and GLUT4, *Drug Des., Dev. Ther.*, 10, 2193–2202.